ROME 2008
LEVERAGING TECHNOLOGY

G024

# Effect of Intrinsic Losses on Seismic Interferometry

D. Draganov* (Delft University of Technology), R. Ghose (Delft University of Technology), E. Ruigrok (Delft University of Technology), J. Thorbecke (Delft University of Technology) & K. Wapenaar (Delft University of Technology)

## SUMMARY

Seismic interferometry (SI) is the process of generating new seismic traces from the cross-correlation of existing traces. One of the starting assumptions for deriving the SI representation equations is that of a lossless medium. In practice, this condition is not always met. Here, we show what the effect is of intrinsic losses on the SI result with the help of a laboratory experiment in a homogeneous sand chamber. Using numerical modelling results, we further show that, in the case of a dissipative inhomogeneous medium with internal multiple scattering, ghost reflections will appear in the cross-correlation results.

## Introduction

In its most general definition, Seismic Interferometry (SI) is the process of generating new seismic traces from the cross-correlation of existing (measured or modelled) traces. SI representation equations can be obtained following different derivation paths. An overview of these paths can be found in the special issue of Geophysics on SI, July-August 2006. All the paths have in common that they start with the assumption of a lossless medium, which means that one can make use of the principle of time-reversal invariance. Of course, when one wants to apply SI to measured laboratory or field data, intrinsic losses cannot be avoided. Using modelling results, Slob *et al.* (2007) showed that for a dissipative medium, composed of two layers, SI still works, but that later arrivals may not be retrieved. Recently, for the case of controlled sources at the surface, Wapenaar *et al.* (2008) proposed to use interferometry-by-deconvolution, i.e., to use deconvolution instead of cross-correlation, where the deconvolution takes also intrinsic losses into account. In the following, we investigate what is the effect of intrinsic losses on the SI cross-correlation results by first testing the modelling results of Slob *et al.* (2007) for the most simple case of a homogeneous medium with laboratory data from a sand chamber and then we show modelling results for an inhomogeneous medium with internal multiples.

## Results for a homogeneous sand chamber

Wapenaar and Fokkema (2006) showed that for an acoustic lossless medium, the SI representation for two-way wavefields can be written as

$$G\left(\mathbf{x}_{\mathcal{A}},\mathbf{x}_{\mathcal{B}},t\right)+G\left(\mathbf{x}_{\mathcal{A}},\mathbf{x}_{\mathcal{B}},-t\right)\approx\frac{2}{\rho c}\oint_{\partial\mathbb{D}}G\left(\mathbf{x}_{\mathcal{B}},\mathbf{x},t\right)*G\left(\mathbf{x}_{\mathcal{A}},\mathbf{x},-t\right)d^{2}\mathbf{x}, \qquad (1)$$

where $G\left(\mathbf{x}_{\mathcal{A}},\mathbf{x}_{\mathcal{B}},t\right)$ denotes the Green's function observed at location $\mathbf{x}_{\mathcal{A}}$ due to an impulsive volume injection-rate density source at $\mathbf{x}_{\mathcal{B}}$, $c$ is the propagation velocity, $\rho$ is the density, and $*$ denotes convolution. Equation (1) shows that by cross-correlating observed Green's functions at locations $\mathbf{x}_{\mathcal{A}}$ and $\mathbf{x}_{\mathcal{B}}$, which result from sources at positions $\mathbf{x}$ on a surface $\partial\mathbb{D}$, one can retrieve the Green's function and its time-reversed version between the locations $\mathbf{x}_{\mathcal{A}}$ and $\mathbf{x}_{\mathcal{B}}$ as if there were a source at $\mathbf{x}_{\mathcal{B}}$ and a receiver at $\mathbf{x}_{\mathcal{A}}$. For a 1-D medium, where the points $\mathbf{x}_{\mathcal{A}}$ and $\mathbf{x}_{\mathcal{B}}$ coincide, one needs to perform auto-correlation. Note that equation (1) holds also for other scalar waves, like SH-waves decoupled from P- and SV-waves.

To investigate the effect of losses on the SI results, we first use a laboratory dataset for a homogeneous medium. The laboratory setup consisted of a sand-filled water-tight cylindrical chamber made of 34 rings, see Fig. 1(a). All the rings were 225 mm in diameter; all the rings were 15 mm thick, except the lowest one, which was 6 mm thick. The sample was prepared through pluviation of sand in water making the sample quite homogeneous. The measurements were performed following a layer stripping method. An SH-wave transducer was placed on the top of the sample, it was set off and the waves transmitted through the loose sand were recorded at the receiver location by a transducer sensitive in a direction parallel to that of the S-wave motion. After this, the top ring was sliced off and a new transmission measurement was performed. Note that this measurement scheme allows us to obtain the wavefield at different heights of the sand by still keeping the medium homogeneous for each height level. The measurements resulted in 34 transmission traces, combined in one panel. This panel exhibits the direct transmission arrival and its multiples (recorded after bouncing between the bottom and the top of the sample); it also exhibits reflections from the walls and their multiples. For our purposes we concentrate on the transmissions. For each source location three different measurements were done by using a source wavelet with a central frequency of 3, 6, and 18 kHz, respectively. From the measurements, we estimated the quality factor of the loose sand in the sample to be around $Q = 16$. This was done using the band-limited (for each source central frequency) spectral ratio of the measurements; the results for the three bands were then averaged. Note that by using a source signal with higher central frequency, effectively we obtain a medium with higher damping. Following equation (1), the transmission panel was auto-correlated. Because

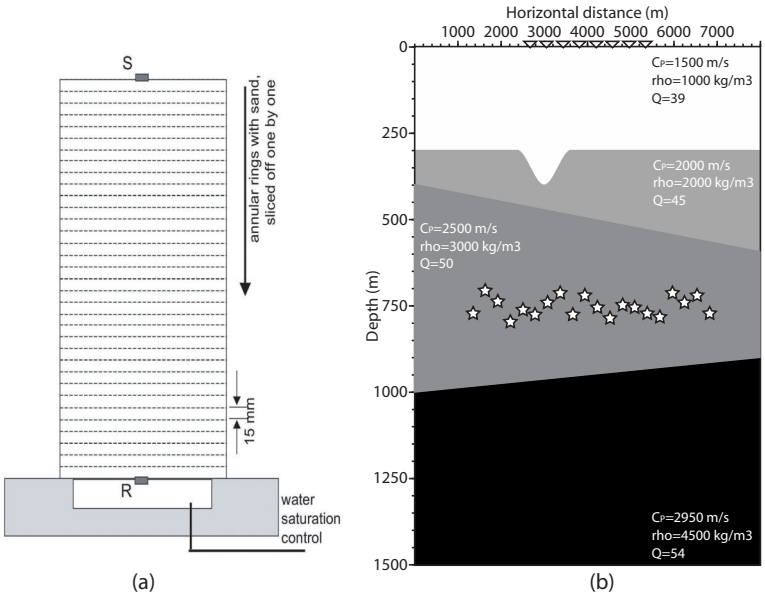


Figure 1: **(a)** A homogeneous sand chamber for measuring transmission responses. S denotes a source of SH-waves and R denotes a receiver sensitive in the direction of the S-wave motion. **(b)** A 2-D dissipative acoustic model used to numerically model transmission and reflection responses. The stars symbolize monopole sources, while the triangles symbolize dipole receivers at the free surface. The sources are randomly spread in the vertical direction between 700 and 850 m, while in the horizontal direction the sources are evenly spread every 25 m from 1200 until 6800 m. The receivers are evenly spread every 10 m between 3000 and 5000 m.

the configuration is close to 1-D, the integral in equation (1) is omitted. The result is a retrieved reflection response of a "vanishing" sand sample, where the source and the receiver are at the same point at the bottom of the sample and after each measurement the top ring is sliced off. Fig. 2(a)-(c) shows the retrieved reflection responses, after muting the negative times, for the vanishing sample for a source signal with 3, 6, and 18 kHz central frequency, respectively. For comparison purposes, in Fig. 2(d) we show the numerically modelled reflection response with coinciding source and receiver at the bottom of the sample with 3 kHz source frequency. We can see that the reflection from the top of the sample is retrieved, but the quality of the retrieved result decreases with increased damping. We can observe the same effect on the multiple reflection (which has bounced two times from the sample's top), but then more notable - in Fig. 2(a) the multiple is readily interpretable, in (b) it is harder to interpret, while in (c) it is nearly invisible. This example shows that in a dissipative medium SI will indeed retrieve the Green's function, but in the case of strong losses the later arrivals may not be retrieved.

**Modelling results for an inhomogeneous medium**

In case of an inhomogeneous medium with internal multiple scattering between the inhomogeneities, like in a layered medium with more that two layers, the problem becomes more complex. For the dissipative acoustic 2-D subsurface model in Fig. 1(b), the directly modelled reflection response with a source at $\mathbf{x}_{\mathcal{B}} = (4000, 0)$ m and receivers at $\mathbf{x} = (3000, 0)$ ... $\mathbf{x} = (5000, 0)$ m is shown in Fig. 3(a). To apply the SI relation (1) to data from this model, we place seismic sources in the subsurface at positions $\mathbf{x} = (1200, z)$ ... $\mathbf{x} = (6800, z)$ m, where $z$ varies randomly between 700 and 850 m, set the sources off one by one and record at the surface the transmitted wavefields resulting from each subsurface source. The separate transmission records are then cross-correlated and summed according to equation (1). Comparing the SI result, shown in Fig. 3(b), to the directly modelled reflection response in 3(a), we see several extra events (ghosts). These ghosts appear due to internal multiples in the transmissions

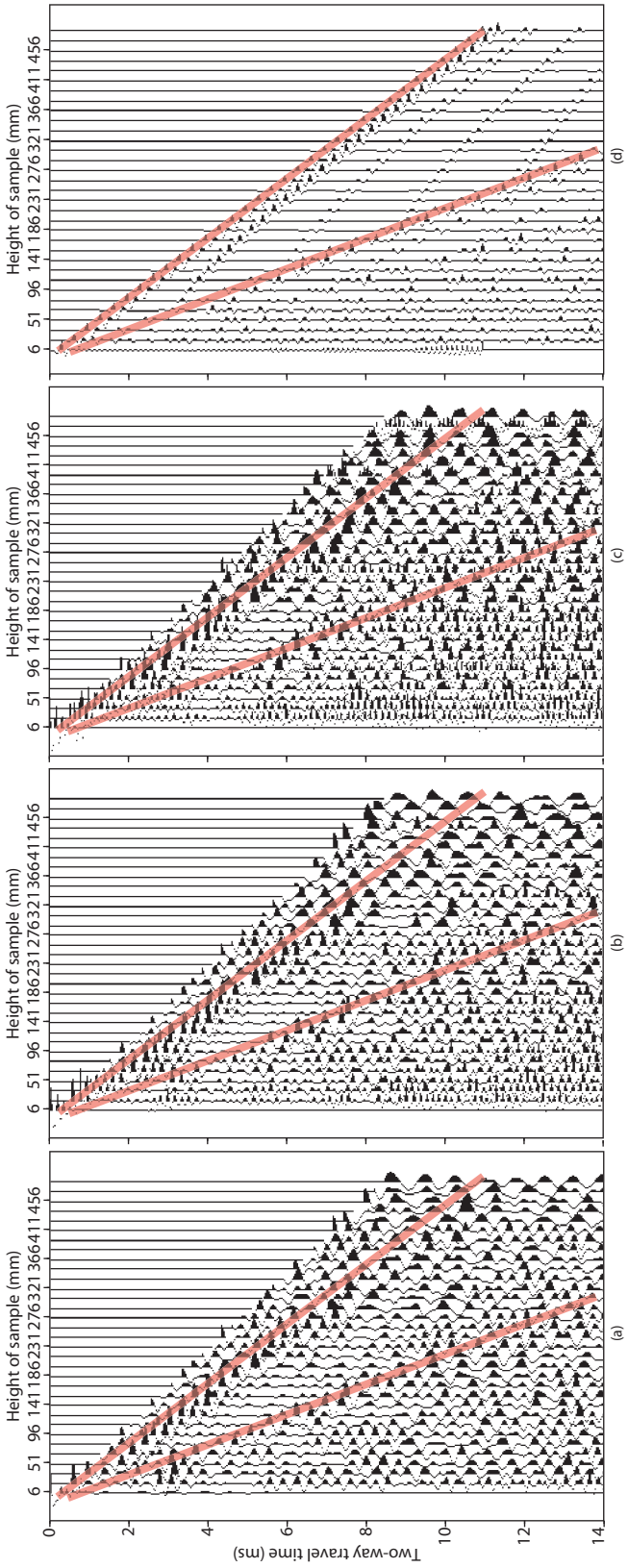


Figure 2: Retrieved reflection response for the sample from Fig. 1(a) for a source signal with central frequency of **(a)** 3 kHz, **(b)** 6 kHz, and **(c)** 18 kHz. **(d)** For interpretation, numerically modelled reflection response for a source signal with 3 kHz central frequency. All four panels are shown after applying AGC with a window length of 4 ms. The two red lines on each panel indicate the place of the reflection from the top of the sample and its first multiple.

(Ruigrok *et al.*, 2008), in our case due to the second and the third layers. In a lossless medium, the internal multiples interfere destructively in the summation process after cross-correlation and do not give rise to ghosts in the SI result. In a dissipative medium, the internal multiples do not interfere destructively anymore and ghosts appear in the SI result. To improve the SI result, a damping compensation should be applied to the transmission records (see Tanter *et al.* (1998) for such an approach). We compensate the damping by multiplying the transmission traces by $exp\,(t\pi f_0/Q)$, where $f_0$ is the source wavelet's central frequency and $Q$ is a constant quality factor. Note that this procedure is valid for transient responses, but not for noise signals. After this processing, the transmission records are cross-correlated and summed (equation (1)). By varying $Q$, we obtain different retrieved reflection responses as shown in Fig. 3(c)-(e). From 3(c), it can be seen that when $Q$ is too high, the ghost events are not completely removed, while from 3(e) it can be seen that when $Q$ is too low the ghost event reappear with reversed polarity. Only when $Q$ is very close to the real values of the quality factors in the second and the third layers, as in 3(d), the ghosts disappear. This shows, that it might be possible to use the damping compensation also as a tool for estimating the Q in the layers.

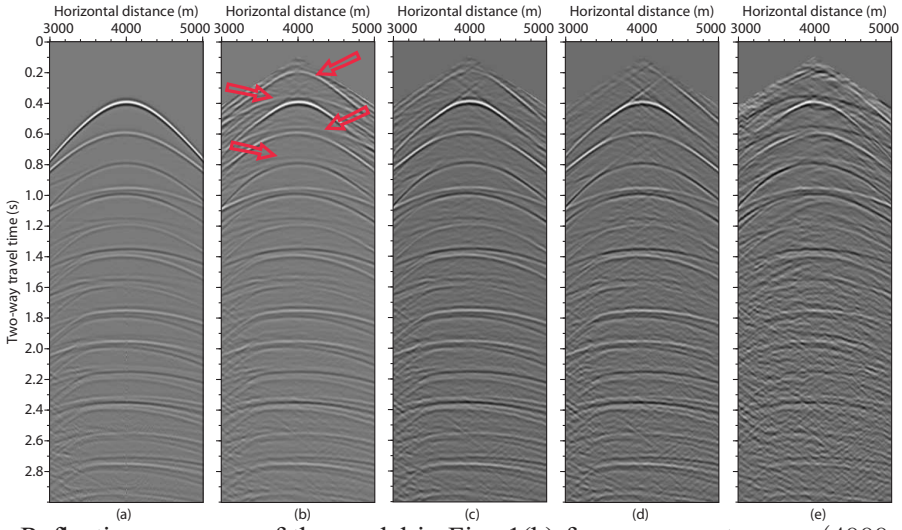


Figure 3: Reflection response of the model in Fig. 1(b) for a source at $\mathbf{x}_{\mathcal{B}} = (4000, 0)$ m and receivers at $\mathbf{x}_{\mathcal{A}} = (3000, z)$ ... $\mathbf{x}_{\mathcal{A}} = (5000, z)$ m: **(a)** Directly modelled; **(b)** Obtained using SI; **(c)** Obtained using SI after damping compensation with $Q = 80$; **(d)** As in (c), but $Q = 45$; **(e)** As in (c), but $Q = 25$ . The red arrows point to ghosts appearing due to the intrinsic losses. All five panels are shown after applying AGC with a window length of 1 s.

## Conclusions

One of the main assumptions in the derivation of Seismic Interferometry representations, based on cross-correlation, is that of a lossless medium. Using transmission responses measured in the ?aboratory on a dissipative homogeneous sand sample, we showed that the cross-correlation result will still retrieve reflections, but some of the later arrivals may not be retrieved. Using numerical modelling results, we showed that in an dissipative inhomogeneous medium with internal multiple scattering the cross-correlation result will give rise to ghost arrivals. These ghosts disappeared after damping compensation was applied to the records before cross-correlation. Using different damping compensation, we showed that it might be possible to estimate the quality factor in the layers that cause the ghosts to appear.

## References

Ruigrok, E., Draganov, D., and Wapenaar, K. [2008] Global-scale seismic interferometry: theory and numerical examples. *Geophysical Prospecting* in press.

Slob, E., Draganov, D., and Wapenaar, K. [2007] Interferometric electromagnetic Green's functions representations using propagation invariants. *Geophysical Journal International* 169, 60–80.

Tanter, M., Thomas, J-L., and Fink, M. [1998] Focusing and steering through absorbing and aberrating layers: Application to ultrasonic propagation through the skull. *Journal of the Acoustic Society of America* 103, 2403–2410.

Wapenaar, K., and Fokkema, J. [2006] Green's functions representations for seismic interferometry. *Geophysics* 71, SI33–SI46.

Wapenaar, K., Slob, E., and Snieder, R. [2008] Seismic and electromagnetic controlled-source interferometry in dissipative media. *Geophysical Prospecting* in press.